DOI: 10.17725/rensit.2023.15.327

Evaluation of images quality obtained by remote sensing

Alexander V. Kokoshkin, Evgeny P. Novichikhin

Kotelnikov Institute of Radioengineering and Electronics of RAS, Fryazinsky branch, http://fireras.su/
Fryazino 141190, Moscow region, Russian Federation

E-mail: shvarts65@mail.ru, epnov@mail.ru

Received March 28, 2023, peer-reviewed April 03, 2023, accepted April 10, 2023

Abstract: **Testing of digital images restoration by methods of sequentially calculated Fourier spectrum interpolation, spline interpolation, projections onto convex sets and amplitude iterations is proposed. The task is a sparseness reconstruction modeled according to the randomly uniform law (90 percent of the information is missing). In addition to the well-known image quality estimates, new ones are introduced - a measure of histogram similarity, the rms deviation of the difference in phase spectra. It is shown that the proposed criteria are effective for assessing the images quality obtained by remote sensing.**

Keywords: **remote sensing, image processing, objective evaluation of the efficiency of reconstruction methods, measure of histogram similarity, standard deviation of phase spectrum difference**

UDC 621.397

Acknowledgments: The work was supported by a state task of the Kotelnikov Institute of Radioengineering and Electronics, Fryazino Branch, Russian Academy of Sciences № 075-01110-23-01.

For citation: Alexander V. Kokoshkin, Evgeny P. Novichikhin. Evaluation of images quality obtained by remote sensing. *RENSIT: Radioelectronics. Nanosystems. Information Technology*, 2023, 15(3):327-334e. DOI: 10.17725/rensit.2023.15.327.

Contents

1. INTRODUCTION

In remote sensing systems, in various ranges of electromagnetic waves, the data obtained are often presented in the form of digital images. When solving practical problems, these images are processed by one method or another. The tasks can be extremely diverse: restoring a defocused partially shaded image, combating noise, increasing spatial resolution, searching for information about a distorting hardware function, reconstructing lost data (lacunae), etc. [1-5]. Thus, an objective assessment of the effectiveness of recovery methods is extremely relevant, since it is an important part of image processing systems obtained with remote sensing.

In this paper, new criteria are proposed for an objective estimate of the quality of reconstructed images relative to the original "ideal" (undistorted). The use of well-known and new objective estimate of image quality makes it possible to assess the competitiveness of image processing methods in remote sensing systems. Here, reconstruction algorithms are applied to sparse images (from unevenly spaced samples). I.e., to such images, over the entire field of which only a certain number of elements are available, while most of the elements are missing. A high degree of sparsity is simulated (90 percent of the information is missing). To restore digital images, methods developed at the V.A. Kotelnikov IRE of the Russian Academy of Sciences are used. In [6,7,8,9], algorithms for the Interpolation Method of Sequential Computation of the Fourier spectrum (IMSCS), the method of projections onto convex sets (POCS) and the method of amplitude iterations (MAI) adapted for the reconstruction of sparse two-dimensional signals were described in detail.

Additionally, as an ideological alternative to methods operating in the frequency domain, spline interpolation is used in our study [10,11]. The physical meaning of this method is that for an arbitrary set of reference points (nodes), a system of linear equations is solved that models the behavior of a curved elastic plate. The result is a relation describing a two-dimensional spline surface. This approach has a certain versatility and can be applied for comparative analysis.

2. APPLICATION OF RESTORATION METHODS TO SPARSE IMAGES

As an example, to illustrate the effectiveness of the methods of reconstruction of sparse images, we use an aerospace image of the aircraft carrier "Midway" moored in the port of San Diego (USA), turned into a museum ship since 1998 (size 1296 by 558 pixels) **Fig. 1**. For this purpose, a public Yandex map is used.

Directly during sparsity modeling and subsequent processing, a fragment of the original image is used in Fig. 1 – the area

Fig. 1. *The original aerospace image (size 1296 by 558 pixels).*

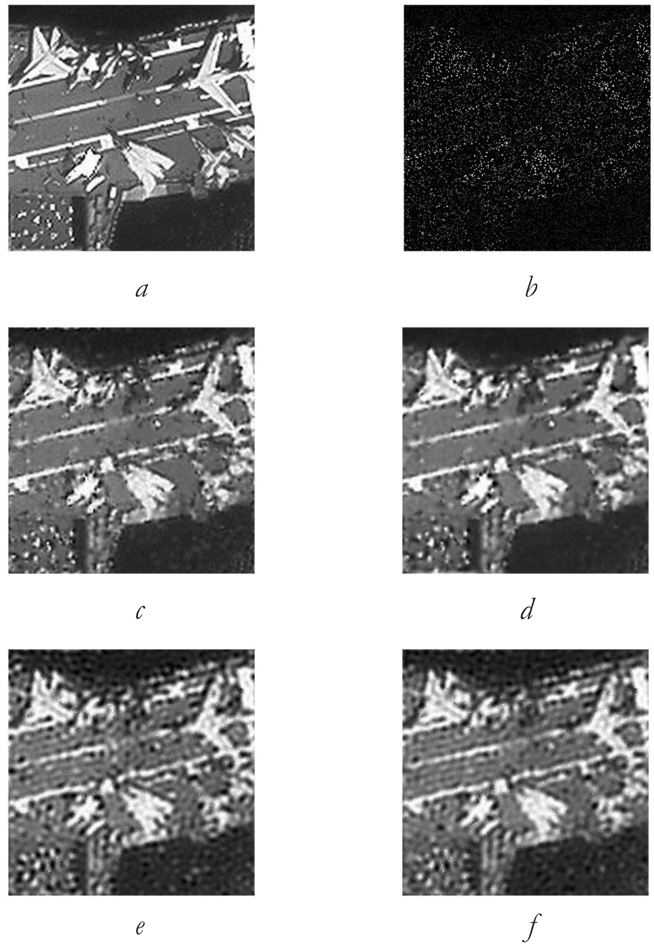

Fig. 2. *Fragment of the original image Fig.1 (size 256 by 256 pixels) – (a); Sparse image (90 percent of the information in Fig. 2a is missing) – (b); Restoration of Fig. 2b) using IMSCS – (c); Restoration of Fig. 2b) using a spline – (d); Restoration of Fig. 2b) using POCS – (e); Restoration of Fig. 2b) using MAI – (f).*

near the stern of the aircraft carrier with a size of 256 by 256 pixels (**Fig. 2***a*). Fig. 2*b* shows a sparse image, where 90 percent of the information is deleted according to a randomly uniform law (black color). Unlike previous works, here, for sparsity modeling (in a Delphi program), a "mask" is used. This makes it possible not to shift the brightness up in order to reserve the "zero" intensity for "places of lack of information", and thus not to make, albeit a small, but compression of the brightness range. Fig. 2*c* shows the restoration of Fig. 2*b* using IMSCS (128 harmonics, 1 iteration). Fig. 2*d* demonstrates the reconstruction of Fig. 2*b* using a spline. The reconstruction of Fig. 2*b* using POCS (a frequency window with a radius of 31 harmonics, 2500 iterations) is shown in Fig. 2*e*. And, finally, the sparsity interpolation of Fig. 2*b* using MAI (frequency window with a radius of 31 harmonics, 2500 iterations) can be seen in Fig. 2*f*.

3. ESTIMATES OF THE RECOVERY QUALITY OF SPARSE IMAGES

An expert observer can visually compare the effectiveness of the methods. The most "similar" to the "ideal" Fig. 2*a* are reconstructions using IMSCS (Fig. 2*c*) and using a spline (Fig. 2*d*). The recovery of a sparse image using POCS (Fig. 2*e*) and using MAI (Fig. 2*f*) is noticeably worse than the first two competing methods. This can be partially explained by a relatively small operating frequency window with a radius of 31 harmonics. The fact is that if you set the frequency window much wider, then on the reconstructed images, in addition to the apparent increase in sharpness, there are significantly more interfering artifacts.

In order to adequately estimate the effectiveness of the methods, it is necessary to calculate the quality criteria. **Table 1** shows objective estimates of the quality of reconstructed images [1,12]: SSIM – Structural Similarity Index Measure, image sharpness evaluation, the average contrast, SD1 is the standard deviation from its average value, SD2 is the standard deviation of the pixel difference between the reference and reconstructed image, excess, asymmetry.

Table 1

Objective estimates of the quality of reconstructed images.

	ideal	IMSCS	spline	POCS	MAI
SSIM	1	0.894	0.895	0.826	0.847
image sharpness evaluation	16.337	8.149	6.264	8.23	7.207
average contrast	0.144	0.114	0.093	0.154	0.13
SD1	66.709	61.19	62.269	63.522	61.719
SD2	0	29.553	29.519	38.44	35.52
excess	-0.101	-0.102	-0.114	-0.354	-0.253
asymmetry	0.88	0.773	0.77	0.643	0.666

The Structural Similarity Index Measure is maximal when comparing the original "ideal" image with itself – it is equal to 1. For all four methods of reconstruction of sparsity, the SSIM are quite close. IMSCS and spline SSIM are almost the same, while POCS and MAI have slightly lower indicators (the worst of all POCS). Nevertheless, POCS shows the "best" result in terms of sharpness estimates. According to this indicator, only IMSCS is nearby. This can be explained by the fact that the assessment of sharpness is strongly influenced by parasitic artifacts (brightness differences compare Fig. 2*c* and Fig. 2*e*). For the same reason, POCS surpasses even the original "perfect" image in "average contrast". Similarly, both estimates of SD systems for POCS are higher than those of competing methods. SD2 (deviation of the pixel difference between the reference and reconstructed image) in MAI noticeably exceed SD2 with IMSCS and spline. This indicates that there are more significant structural differences with the "ideal" images of restored POCS and MAI than in IMSCS and spline reconstructions. The excess of the brightness values for a digital image indicates how flat or insular the distribution is when compared with the normal distribution. The fact that the calculated excess values for all images are less than zero indicates that all distributions are flat-topped (relative to the normal, whose excess is zero). As for the absolute values of the excess for the studied methods, IMSCS is the closest to the original one.

The asymmetry of the brightness values for a digital image measures the asymmetry of the distribution near the average. Positive values of asymmetry for all four methods indicate that the "tail" of the distribution is stretched in the direction of positive values. If the asymmetry of the image brightness values were zero, then the distribution would be symmetrical about its average (as in the case of normal). According to this indicator, the method of interpolation of the sequentially calculated Fourier spectrum surpasses competitors in this study – it is closer to the "ideal" one.

After analyzing the data in Table 1, it can be stated that according to the objective estimates of the quality of reconstructed images calculated above, IMSCS has some advantage over competing methods. The expert assessment also leans towards the interpolation method of the sequentially calculated Fourier spectrum. In [13], another objective quality criterion was introduced. As can be seen from the Table.1 some of the assessments may produce contradictory results. It is proposed to compare the forms of brightness distributions of reconstructed images with a similar distribution for the reference. This is practically implemented on histograms. Moreover, the histograms need to be "coarsened" a little, i.e. not to take them for all brightness gradations (256), but to calculate averaged, for example, 8 (we get 32 columns in each histogram). This is due to the fact that the pixels of some of the brightness gradations may be physically absent from certain images [13]. **Fig. 3** illustrates the normalized brightness histograms of the images under discussion.

Fig. 3*b* indicates an extremely small amount of significant information (10 percent) present in the sparse image. Upon closer examination of Fig. 3, it can be seen that the type of histograms varies significantly for different sparsity interpolation methods. And if each of them is numerically compared with the "standard" (Fig. 3*a*), then an objective criterion for evaluating the quality of images will be obtained. By analogy with the already known structural similarity index measure (SSIM), we will call it "histogram similarity index measure" (HSIM) [13].

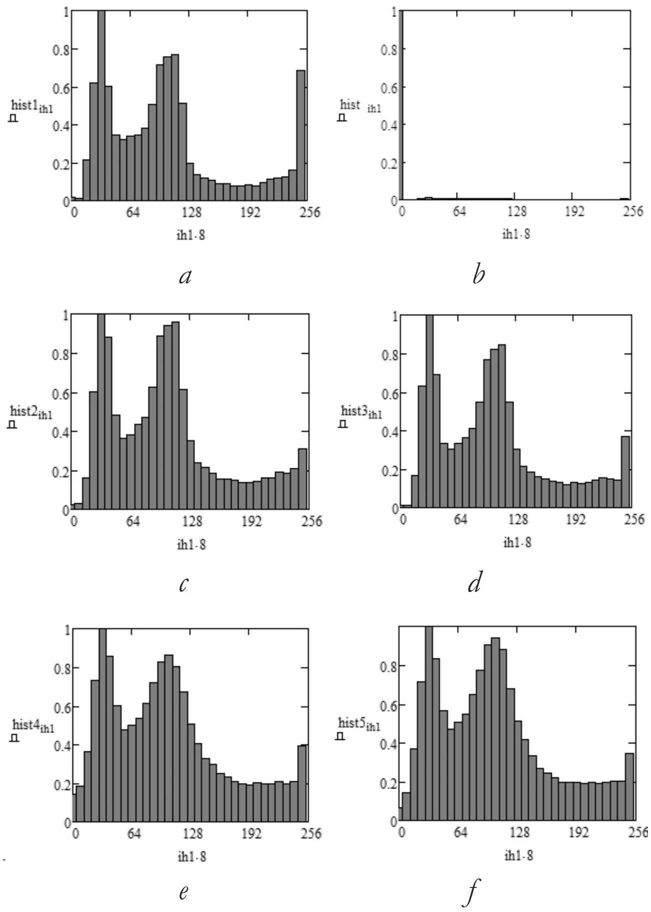

Fig. 3. *Brightness histograms for: the original image Fig. 2a) – (a); sparse image Fig. 2b) – (b); restored Fig. 2c) using IMSCS – (c); restored Fig. 2d) using a spline - (d); restored Fig. 2b) using POCS – (e); restored Fig. 2b) using MAI – (f).*

It is proposed to calculate the measure of histogram similarity as follows [13]:

$$\mathbf{HSIM} = \frac{\sum_{\mathbf{ih1}=0}^{31} \left|\mathbf{hist1}_{\mathbf{ih1}} - \mathbf{hist2}_{\mathbf{ih1}}\right|}{32}.$$

In this formula: $\text{hist1}_{\text{ih1}}$ – values along the columns of the reference normalized histogram (Fig. 3*a*); $\text{hist2}_{\text{ih1}}$ – values for the columns of the normalized histogram under test (Fig. 3*c*). The averaged modulus of the difference is calculated for each pair of histogram bars. In the proposed example, 32 is equal to the number of bars in the histograms (256 divided by 8). So the above formula calculates the HSIM for IMSCS. Similar are calculated histogram similarity index measure to the spline while substituting in the formula as a test histogram values $\text{hist3}_{\text{ih1}}$ (Fig. 3*d*), for POCS, substituting in the formula $\text{hist4}_{\text{ih1}}$ (Fig.

Table 2

Histogram similarity index measure

	ideal	IMSCS	spline	POCS	MAI
HSIM for normalized histograms	0	0.094	0.049	0.153	0.157
HSIM for non-normalized histograms	0	360.625	266.875	583.688	547.875

3*e*), or hist5$_{ih1}$ (Fig. 3*f*) when calculating the HSIM to MAI. **Table 2** shows the histogram similarity index measure calculated according to the proposed method for the studied images. HSIM for the original (reference) image, in our case, means comparison with itself, so the difference in values is zero [13].

When evaluating sparsity reconstructions by various methods, spline has an advantage over competitors, IMSCS is in second place. Most significantly (in percentage terms) this is manifested if data from normalized histograms are used for calculations.

Fig. 4 shows the amplitude spatial spectra on a logarithmic scale: the original ("ideal") image (Fig. 2*a*) – Fig. 4*a*; sparse image (Fig. 2*b*) – Fig. 4*b*; sparsity reconstruction using IMSCS (Fig. 2*c*) – Fig. 4*c*; sparsity reconstruction using a spline (Fig. 2*d*) – Fig. 4*d*; sparsity reconstruction using POCS (Fig. 2*e*) – Fig. 4*e*; reconstruction of sparsity using MAI (Fig. 2*f*) – Fig. 4*f*. Vertically Fig. 4 the values of the amplitudes of the spatial spectra are postponed (on a logarithmic scale), along the other axes – the values of the indices of brightness pixels in the image field.

In [1] it is stated: the amplitude of a two-dimensional discrete Fourier transform is an array whose components set the intensities in the image, and their corresponding phases make up an array of offsets, which contains a significant part of the information about where visible objects are placed in the image. Thus, the basic information about the contours (details) of objects in the images is contained in the phase spectrum. In this connection, the idea arises of

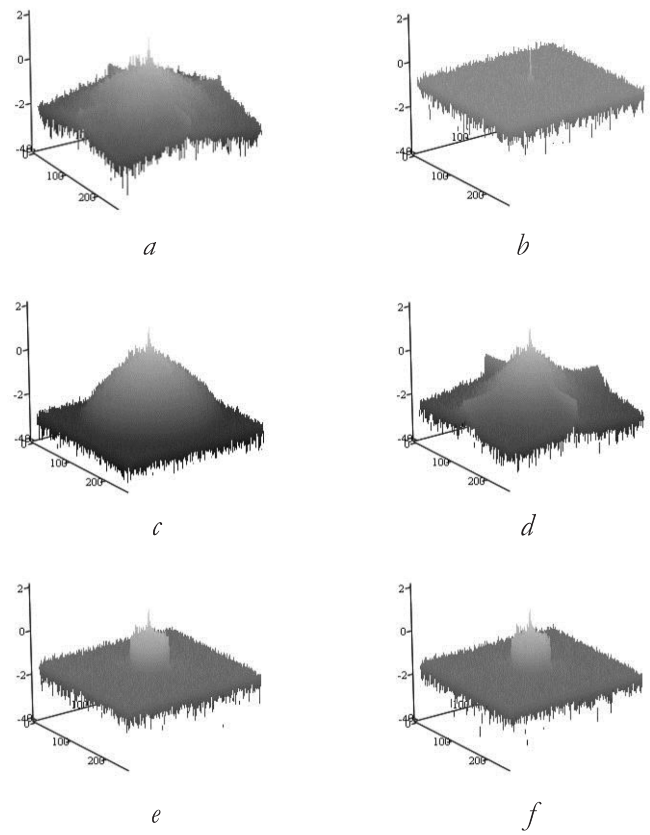

Fig. 4. *Amplitude spatial spectra in logarithmic scale for: the original image Fig. 2a) – (a); sparse image Fig. 2b) – (b); restored Fig. 2b) using IMSCS – (c); restored Fig. 2b) using a spline - (d); restored Fig. 2b) using POCS – (e); restored Fig. 2b) using MAI – (f).*

creating some kind of objective criterion for assessing the quality of the phase spectrum of the reconstructed images. Visually, the phase spectrum of images is difficult to interpret in any way. **Fig. 5***a* shows the phase spectrum of the original "ideal" image, and Fig. 5*b* shows the spectrum of a sparse image. Vertically, Fig. 5 shows the values of the phase of spatial spectra

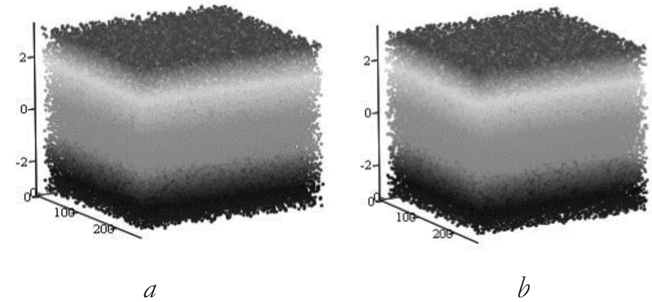

Fig. 5. *The phase spatial spectra of the value are in the range (-π , π]: of the original image Fig. 2a) – (a); of the sparse image Fig. 2b) – (b).*

(in the interval (–π, π]), along the other axes – the values of the indices of brightness pixels in the image field.

We propose to calculate pixel-by-pixel the differences in the phase spatial spectra between the original ("ideal") and sparse images (see Fig. 5). The array of values of the result of the operation is in the range (-2π , 2π]. All similar arrays for the difference of phase spatial spectra between the original ("ideal") and any of the four images reconstructed by the methods studied here should have a smaller spread of values. **Fig. 6** shows sections of arrays of values: the phase spectrum of the "ideal" image minus the phase spectrum of the sparse image Fig. 6*a*, and the phase spectrum of the "ideal" undistorted source image minus the phase spectrum of sparsity restoration using IMSCS Fig. 6*b*. Vertically Fig. 6, the values of the phase difference of spatial spectra are postponed (in the interval

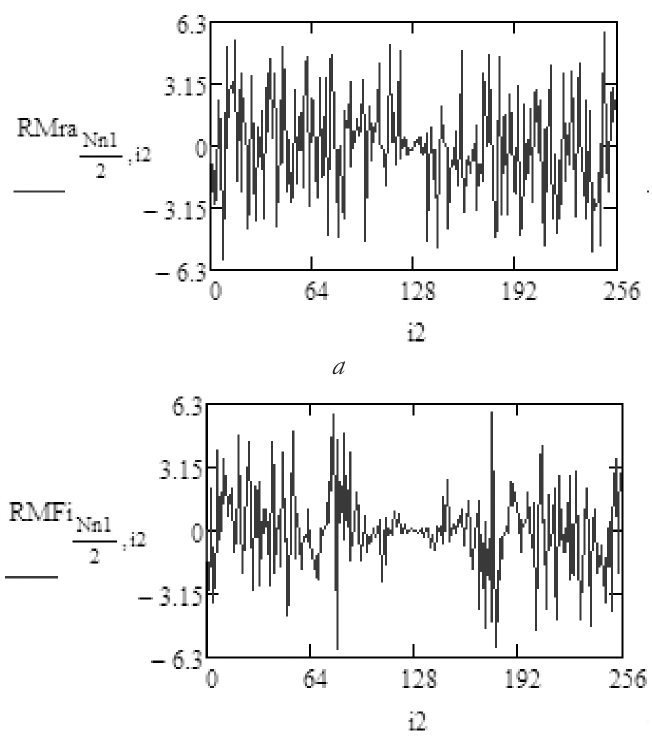

Fig. 6. *Sections of the difference of the full phase spatial spectra: the "ideal" undistorted source image (Fig. 2a) minus the phase spectrum of the sparse image (Fig. 2b) – (a); the "ideal" undistorted source image (Fig. 2a) minus the phase spectrum of sparsity recovery using IMSCS (Fig. 2c) – (b).*

Table 3

SD of the difference of phase spectra (in rad.) between the "ideal" and reconstructed images

	ideal	sparse	IMSCS	spline	POCS	MAI
SD for the full spectrum	0	2.529	2.423	2.362	2.442	2.438
SD for the central part of the spectrum (with a radius of 31 harmonics)	0	0.893	0.63	0.641	0.714	0.701

(–2π, 2π]), horizontally – the values of pixel brightness indices in the image field.

Fig. 6 shows that near the central frequency of the spectrum (corresponding to the average brightness of the image), the phase differences are relatively small. But as we move away into the high frequency region, the values of the phase difference increase on average. In the first row of **Table 3**, the phase differences for the full spectrum between the "ideal" and the reconstructed images considered here by the methods are given.

The results for a sparse image are obviously the worst. The ratio of the difference of the phase spectra (in rad.) of the "ideal" image with itself is an array of zeros (the first column of Table 3), i.e. the best result. In order to put competing methods in more equal conditions, we limit the calculation of the difference between the phase spectra to a region near the central frequency with a radius of 31 harmonics. This corresponds to the frequency window size chosen in this paper for POCS and MAI.

Fig. 7 shows the corresponding sections for the central zones (with a radius of 31 harmonics) of the difference in the phase spatial spectra.

Table 3, in the second line, shows the values of the SD for the central part of the spectrum (with a radius of 31 harmonics) of the difference in phase spectra (in rad.) between the "ideal", sparse and reconstructed images. According to this indicator, IMSCS takes the first place, the second is spline, the third is MAI, and the last is POCS.

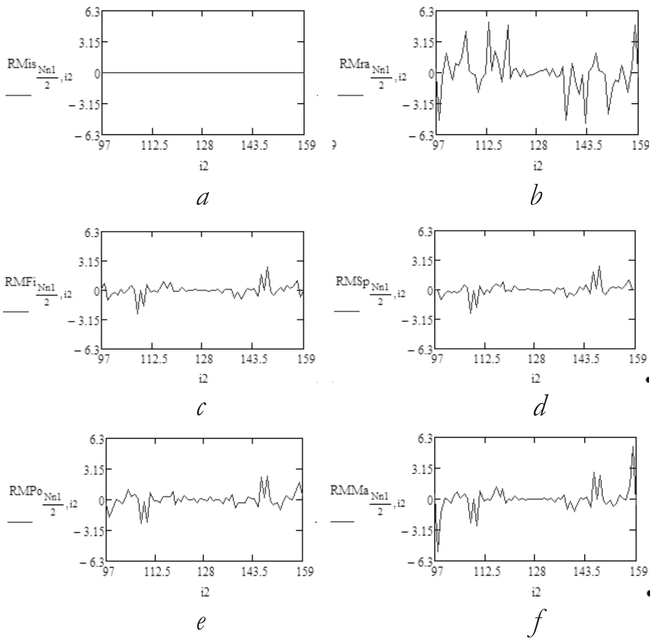

Fig. 7. *Sections for the central zones (with a radius of 31 harmonics) of the difference in the phase spatial spectra: the "ideal" undistorted source image (Fig. 2a) minus the phase spectrum of itself – (a); the "ideal" undistorted source image (Fig.2a)) minus the phase spectrum of the sparse image (Fig. 2b) – (b); "ideal" undistorted source image (Fig. 2a) minus the phase spectrum of sparsity recovery using IMSCS (Fig. 2b) – (c); "ideal" undistorted source image (Fig. 2a) minus the phase spectrum of sparsity restoration using a spline (Fig. 2d) – (d); "ideal" undistorted source image (Fig. 2a) minus the phase spectrum of sparsity restoration using POCS (Fig. 2e) – (e); "ideal" undistorted source image (Fig. 2a) minus the phase spectrum of sparsity recovery using MAI (Fig. 2f) – (f).*

4. CONCLUSION

The paper proposes new objective assessments of the quality of images obtained by remote sensing (the histogram similarity index measure, the SD of the difference in phase spectra). The following methods are used as tested methods: the Interpolation Method of Sequential Computation of the Fourier Spectrum (IMSCS), spline interpolation, the method of projections onto convex sets (POCS) and the method of amplitude iterations (MAI). Competing methods reconstructed the sparsity modeled according to a randomly uniform law (90 percent of the information is missing). IMSCS showed the best performance in almost all estimates. The conducted research allows us to conclude that the proposed criteria can be applied in principle to assess the quality of images obtained by remote sensing. This allows you to check the effectiveness of digital image recovery methods used to solve various practical problems.

REFERENCES

1. Gonzalez RC, Woods RE. *Digital Image Processing*. International Version 3rd Edition. NJ, Prentice Hall, 2012, 1071p.
2. Huang H, Makur A. A new iterative reconstruction scheme for signal reconstruction. *Proceedings of the IEEE Asia Pacific Conference on Circuits and Systems* (*APCCAS '08*). 2008; https://doi.org/10.1109/APCCAS.2008.4746028.
3. Zrazhevsky AY, Kokoshkin AV, Korotkov VA, Korotkov KV. Vosstanovlenie defokusirovannogo zatenennogo izobrazheniya [Recovery of defocusing partially shaded image]. *Zhurnal radioelektroniki* [*Journal of Radioelectronics*] [online]. 2014, №10, http://jre.cplire.ru/jre/oct14/9/text.html (in Russ.).
4. Kokoshkin AV. Features of an Application of the Constrained Renormalization Method to Images with Speckle Noise. *J. of Communications Technology and Electronics*, 2022, 67(12):1419-1429. DOI: 10.1134/S1064226922120075.
5. Kokoshkin AV, Korotkov VA, Novichikhin EP. Comparison of interpolation methods when achieving super-resolution of images based on the analysis of several frames. *RENSIT: Radioelectronics. Nanosystems. Information Technologies*, 2019, 11(1):85-91. DOI: 10.17725/rensit.2019.11.085.
6. Kokoshkin AV, Korotkov VA, Korotkov KV, Novichikhin EP. Retouching and restoration of missing image fragments by means of the iterative calculation of their spectra. *Computer Optics,* 2019; 43(6):1030-1040. DOI: 10.18287/2412-6179-2019-43-6-1030-1040.
7. Kokoshkin AV, Korotkov VA, Novichikhin EP. Reconstruction of Acoustic Signals

According to Incomplete Data. *J. of Communications Technology and Electronics,* 2020, 65(12):1399-1406. DOI: 10.1134/S1064226920120104.

8. Kokoshkin AV, Novichikhin EP. Application of the Interpolation Method of Sequential Computation of the Fourier Spectrum to Sparse Images. *RENSIT: Radioelectronics. Nanosystems. Information Technologies*, 2022, 14(2):165-174e. DOI: 10.17725/rensit.2022.14.165.
9. Kokoshkin AV. Algoritmy metoda amplitudnykh iteratziy i POCS dlya rekonstruktsii razrezhennykh dvumernykh signalov [Algorithms of the method of amplitude iterations and POCS for the reconstruction of sparse two-dimensional signals]. *Zhurnal radioelektroniki* [*Journal of Radioelectronics*] [online]. 2022, №9; https://doi.org/10.30898/1684-1719.2022.9.7 (in Russ.).
10. Ashkenazy AV. *Spline surfaces. Fundamentals of the theory and computational algorithms.* Tver, Tver State University Publ., 2003, p. 82.
11. Nesterenko EA. Vozmozhnost' ispol'zovaniya splainpoverkhnosti dlya postroeniya poverkhnostey po rezultatam c'emok [The ability to use spline surfaces for constructing surfaces based on the shooting results]. *Zapiski Gornogo Instituta,* 2013, 204:127-133 (in Russ.).
12. Kokoshkin AV, Korotkov VA, Korotkov KV, Novichikhin EP. Sravnenie ob'ektivnykh metodov ozenki kachestva zifrovykh izobrazheniy [Comparison of objective methods of assessing quality of digital images]. *Zhurnal radioelektroniki* [*Journal of Radioelectronics*] [online]. 2015, №6; http://jre.cplire.ru/jre/jun15/15/text.html (in Russ.).
13. Kokoshkin AV. Metody interpolyatsii razrezhennykh izobrazheniy, rabotayushchie v chastotnoy oblasti [Sparse Image Interpolation Methods Working in the Frequency Domain]. *Zhurnal radioelektroniki* [*Journal of Radioelectronics*] [online]. 2023, №3; https://doi.org/10.30898/1684-1719.2023.3.10 (in Russ.).